Ecological Indicators 176 (2025) 113614

Contents lists available at ScienceDirect

Ecological Indicators

journal homepage: www.elsevier.com/locate/ecolind

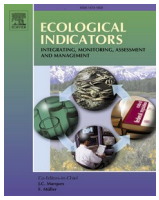

Identifying landscape patterns at different scales as driving factors for urban flooding

Yao Li [a,*], Frank Badu Osei [a], Shaoqing Dai [b], Tangao Hu [c,d], Alfred Stein [a]

[a] Faculty of Geo-Information Science and Earth Observation (ITC), University of Twente, 7500 AE Enschede, the Netherlands
[b] School of Resource and Environmental Sciences, Wuhan University, 129 Luoyu Road, Wuhan 430079, China
[c] School of information science and technology, Hangzhou Normal University, Yuhangtang Road No. 2318, Hangzhou 311121, China
[d] Institute of Remote Sensing and Earth Sciences, Hangzhou Normal University, Yuhangtang Road No. 2318, Hangzhou 311121, China

ARTICLE INFO

Keywords:
Urban flooding
Driving factor
Landscape composition and configuration
Scale effect

ABSTRACT

Climate change and rapid urbanization have led to increasingly frequent urban flooding, causing substantial losses. While previous studies have examined the impact of land use types on flooding, few studies have explored how the spatial distribution and configuration of land use (landscape patterns) influence urban flooding across different scales. This study addresses this gap by investigating the effects of landscape patterns on urban flood events in Chengdu, China. We constructed a comprehensive dataset comprising 28 flood influencing factors, including landscape pattern, topographic, and hydrological characteristics. Using Principal Component Analysis (PCA), we classified these variables and applied stepwise Poisson regression to evaluate how landscape patterns affect urban flooding. Our findings show that key influencing factors vary by scales: at the 1 km scale, topographic factors were most important; at the 2 km scale, impervious areas had the largest impact; and at the 3 km scale, landscape configuration factors were dominant. In particular, the mean patch area and cohesion were consistently significant across all scales, indicating that more fragmented and dispersed landscapes tend to reduce flooding occurrence. We conclude that scale is an important determinant for properly understanding the contribution of landscape patterns to urban flood mitigation.

1. Introduction

The frequency, intensity, and severity of hydro-meteorological events have significantly increased in recent decades due to global climate change, leading to an increase in extreme flooding events (Li et al., 2024; Nearing et al., 2024). By now, the number of people affected by floods is nearly equivalent to that of all other natural disasters combined (Ali et al., 2022; Birkholz et al., 2014). One reason is that rapid urbanization has led to the expansion of impervious surfaces, disrupting the natural surface water cycle and further exacerbating the urban flood risk (Wang et al., 2023b). As evidenced by the historic rainfall of 624.1 mm (Li et al., 2023b) on July 20, 2021, in Zhengzhou city, the consequences of the flooding were catastrophic, including the loss of 398 lives and economic damages totaling RMB 65.5 billion (Zheng et al., 2022). Consequently, addressing urban flooding has emerged as a critical issue for advancing resilient community construction in China.

Urban flooding occurs in urban areas where heavy or continuous rainfall leads to serious waterlogging on roads and low-lying areas due to inadequate drainage and infiltration capacity (Zhang et al., 2021). Although underground drainage pipe networks can mitigate urban flooding to some extent (Li et al., 2024), improvement of the drainage system infrastructure is expensive (Chen et al., 2021; Davis & Naumann, 2017). From the perspective of urban planning, investigating the impact of different surface environments on urban flooding and developing disaster prevention strategies, are highly significant for reducing economic losses and improving the safety of residents' lives and property (Zimmermann et al., 2016).

Climate change and rapid urbanization have profoundly altered hydrological cycles in cities (Sun et al., 2023; Zhang et al., 2022), leading to increased rainfall intensity, reduced infiltration, and accelerated runoff production (Ma et al., 2024). Urban expansion often replaces natural land covers with impervious surfaces (Pan et al., 2023), amplifying surface runoff and reducing water retention capacity (Ma et al., 2022). Previous research has highlighted the impact of impervious surfaces on urban flooding (Wang et al., 2022). Those areas play a

* Corresponding author.
E-mail address: yao.li@utwente.nl (Y. Li).

https://doi.org/10.1016/j.ecolind.2025.113614
Received 20 September 2024; Received in revised form 29 April 2025; Accepted 15 May 2025
Available online 23 May 2025

critical role in influencing flooding by affecting water flow, flood propagation, flow volume, and peak flow (Sohn et al., 2020). Recent studies emphasized that the impact of floods is also influenced by the overall characteristics of the landscape (Zhang et al., 2020). Two landscape ecological concepts have been used so far (Karimi et al., 2021): landscape composition as the proportions of different land use types within a specific landscape unit; and landscape configuration described as the spatial arrangement of landscape units (Osborne & Alvares-Sanches, 2019). While the influence of landscape composition on flooding is well-studied, there has been limited research on the impact of landscape configuration (Wang et al., 2023a).

Most studies have focused on single-scale (Li and Bortolot, 2022) or single-factor (Sohn et al., 2020) analyses, overlooking their complex interactions and scale effects. In heterogeneous urbanized areas, multi-scale analysis is essential (Saura & Castro, 2007). The concept of scale effect originates from landscape ecology. It indicates that landscape elements exhibit varying characteristics at different spatial scales. Understanding the landscape structure in the context of spatial heterogeneity also requires multiscale information (Rahimi et al., 2021). The scale effect is an important factor that relates to the complexity of landscape phenomena (Šímová and Gdulová, 2012). A single-scale analysis can provide partial information about landscape characteristics, while considering multiple scales can reveal the complex relationship between urban flooding and regulating factors. Considering the scale effect can also help us to better understand how environmental factors affect urban flooding.

This study aims to develop a novel multiscale and multifactor framework to analyze the complex mechanisms driving urban flooding. We focused on the urbanized central Chengdu area, known for its susceptibility to flooding (Li et al., 2023a). We employed a stepwise Poisson regression model to quantify the complex relations between urban flooding and influencing factors at different spatial scales. Our research is driven by a set of research questions that aim to shed light on the causes of urban flooding: (1) How do changes in scales affect the variation of influencing factors? (2) How do landscape pattern factors influence urban flooding across different scales? (3) What dominant factors cause flooding to occur and at what scale? In this way, a better understanding will be obtained of how urban flooding interacts with the features of our cityscapes, thereby developing effective urban planning strategies to mitigate flood risks.

2. Materials and methodology

2.1. Study area and research framework

Chengdu is the capital city of Sichuan Province (Fig. 1b) and the largest city in southwestern China (Fig. 1a), covering an area of 3,640 km^2. Its resident population according to the seventh national census in 2021 reported a permanent population close to 21 million. Chengdu has a subtropical monsoon climate with abundant rainfall in summer. With its rapid urbanization and city expansion, Chengdu is facing increasingly serious urban flooding issues during the summer. Considering the high risk of urban flooding events in this region, it is representative to identify the influencing factors of urban flooding. Our focus is on the municipal districts that were affected by recurrent flood disasters, as shown in Fig. 1c.

This study utilized terrain data, remote sensing imagery, and land use data to construct a database of surface influence factors. A Digital Elevation Model (DEM) was obtained from ASTER GDEM V2 at a 30 m resolution from the Geospatial Data Cloud platform (https://www.gscloud.cn). Sentinel-2 images were acquired and processed through the Google Earth Engine Platform (https://earthengine.google.com). Land use data were obtained from the global land use/land cover (LULC) dataset developed by Gong et al., (2020), which derived from Sentinel-2 images (10 m resolution) and generated annually using a deep learning classification model trained on billions of manually labeled image pixels. Administrative division data in Shapefile format were provided by the Chengdu Civil Affairs Bureau. All datasets were clipped according to administrative division boundaries to ensure consistent processing areas. Flooding data originated from the Weibo platform and were validated as reported previously (Li et al., 2023). A summary of the datasets is provided in Table 1.

To provide a clear overview of the analytical process, Fig. 2 presents the research workflow. After collecting the datasets including flood inventory and fundamental datasets, we determined the analysis scales. Then, influencing factors were classified into four categories: landscape composition, landscape configuration, topographic, and hydrological factors. We applied Principal Component Analysis (PCA) to reduce dimensionality and stepwise Poisson regression to identify key flood-driving factors. Finally, scale-specific flood management strategies were developed based on the analysis results.

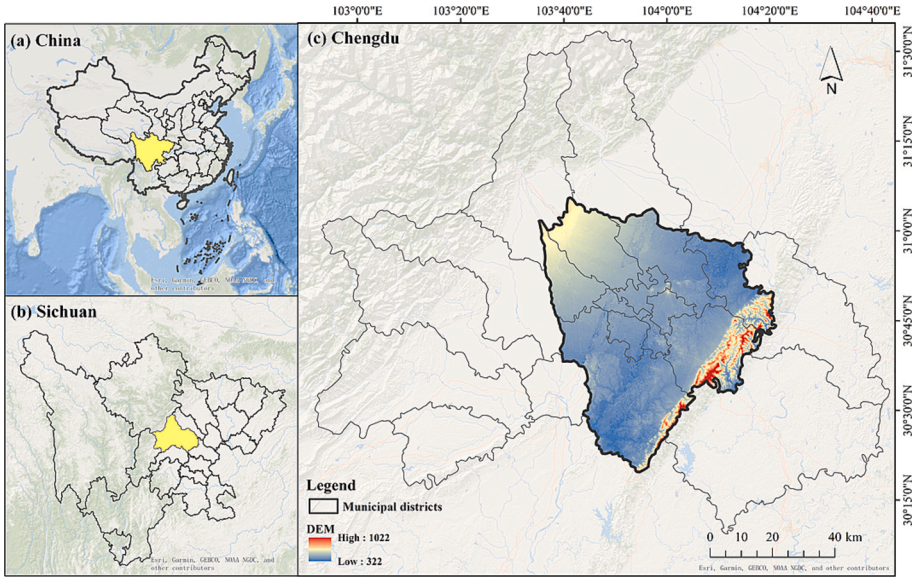

Fig. 1. Study area: (a) Sichuan province located at the southwestern China; (b) Chendu city situated in the central part of Sichuan province; and (c) the municipal districts of Chengdu city.

Table 1
Datasets used in this study.

Data and format	Spatial resolution	Time	Source
Flood records (Shapefile)	Point	July 2018	Social Media data from Weibo
Topographic data (Raster)	30 *m*	–	ASTER GDEM V2
Administrative boundaries (Shapefile)	Polygon	2018	Chengdu Civil Affairs Bureau
Sentinel 2 images (Raster)	10 *m*	2018	Google Earth Engine Platform
River (Shapefile)	Polygon	2018	National Catalogue service For Geographic Information

2.2. Determination of analysis scales

The selection of analysis scales was based on both national urban planning standards and data limitations. According to the Construction and Application Regulations for Urban Flood Control System formulated by the China Association for Engineering Construction Standardization, the minimum planning unit is 1 km^2. Therefore, we adopted 1 km as the minimum scale (Fig. 3a). Considering the limited sample size of urban flooding events, the maximum analysis scale was set at 3 km. Consequently, we defined three analysis scales: 1 km (S1), 2 km (S2), and 3 km (S3). These scales therefore correspond to different levels of urban spatial organization: the 1 km scale to localized drainage patterns and micro-topographic variations; the 2 km scale to neighborhood-level urban structures; and the 3 km scale to broader landscape patterns that influence surface water accumulation and flooding.

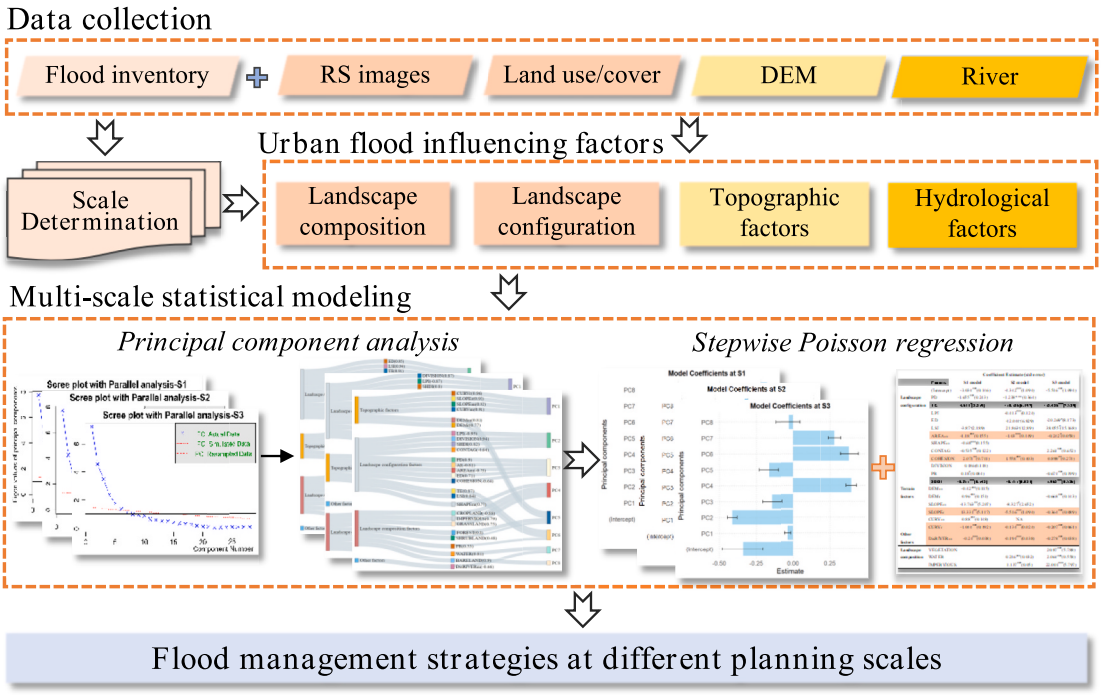

Fig. 2. Research framework.

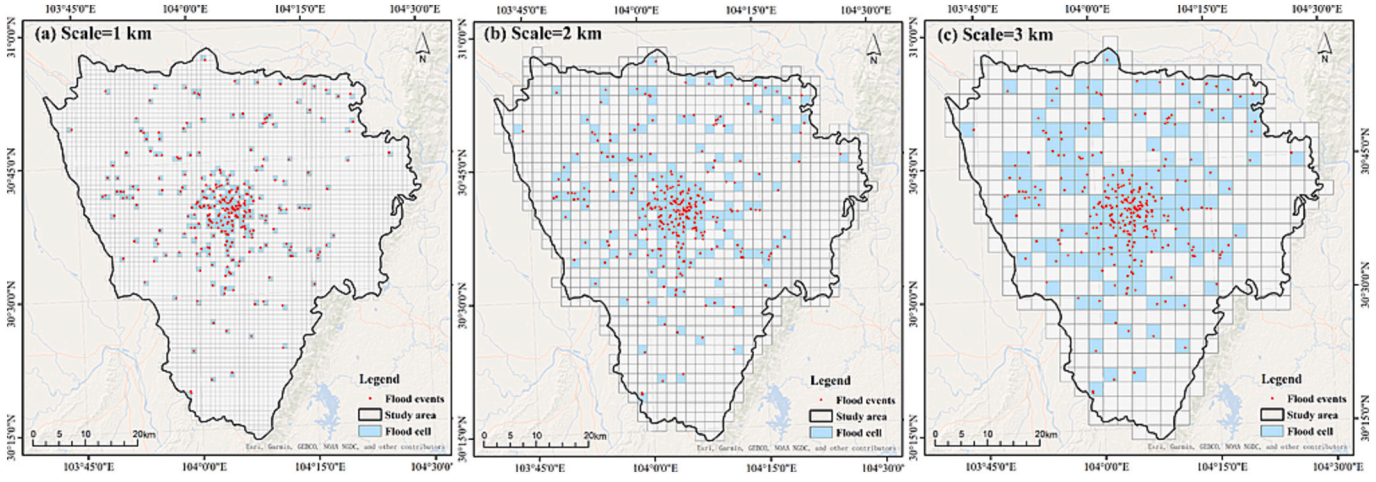

Fig. 3. Analysis scales.

2.3. Urban surface influencing factors

Landscape characteristics refer to the spatial arrangement of land cover within a landscape. It encompasses landscape composition, defined as the quantity of each land cover or land use type, and landscape configuration, defined as the spatial patterns and connectivity of these types (Karimi et al., 2021). In landscape ecology, a variety of metrics can be used to quantify landscape configuration at the patch, class, and landscape levels. As shown in Fig. 4, a patch is the smallest landscape unit, while a class refers to the overall characteristics of a specific land cover type. The focus of our study is on the landscape level, which refers to the spatial patterns and processes of an entire landscape, including patches and classes.

We collected 28 influencing factors and categorized them into four groups: 9 landscape composition factors, 12 landscape configuration factors, 6 topographic factors, and 1 other factor. The definitions, expressions, and ecological description of each flood influencing factor are detailed in Table 2.

(1) Landscape composition factors quantify the variety and abundance of land cover types within a landscape. These factors influence water infiltration and runoff processes, thereby affecting the extent of urban flooding. To characterize landscape composition, we use Patch Richness (PR) and the percentage of the landscape type (P_i).

(2) Landscape configuration factors assess the spatial arrangement, shape, and pattern of the land cover patches. They play a critical role in water exchange and circulation which impacts the severity of urban flooding. For example, the Largest Patch Index (LPI) reflects the dominance of a single patch, with higher values indicating lower fragmentation (Zou et al., 2022); Total Edge (TE) measures the degree of edge complexity, affecting how water flows across patch boundaries (Kuo et al., 2021); the Aggregation Index (AI) quantifies spatial continuity and physical connectedness of patches, which influence surface runoff and infiltration potential (Yin et al., 2025); and Shannon's Diversity Index (SHDI) captures landscape diversity and heterogeneity, being closely linked to water retention capacity and flow redistribution (Li et al., 2021). By interpreting these metrics, we gain ecological insight into how landscape structure regulates hydrological responses such as runoff generation and flood propagation. For this study, we selected 11 key factors, including 2 edge factors: TE and Edge Density (ED); two patch size factors: LPI and Mean Patch Area (AREAm); four contagion/interspersion factors: AI, Contagion (CONTAG), Landscape Shape Index (LSI), and Patch Cohesion Index (COHESION); two subdivision factors: Patch Density (PD) and Landscape Division Index (DIVISION); and one diversity factor: SHDI. We employed the Fragstats 4.2 software (https://www.fragstats.org) to obtain the landscape configuration metrics. A moving window method was used, with window sizes according to the defined scales set at 1 km, 2 km, and 3 km, respectively. This allowed us to make localized assessments of landscape patterns for each analysis unit. All landscape metrics were computed at the landscape level, ensuring that the resulting indices accurately captured the spatial composition and configuration that are relevant to urban flood analysis.

(3) Topographical variables can influence the distribution and flow paths of surface runoff within a city. Elevation affects the direction of water flow; slope impacts the speed of water flow; and curvature influences the convergence and dispersion of water. Here, we selected six key topographic factors, including the mean and range values of elevation, slope, and curvature within each landscape unit. The mean values provide an overview of the overall terrain characteristics, while the range values indicate the extent of variability within the landscape unit.

(4) Hydrological factor: Distance to the river (DisRIVERm) was included, as proximity to rivers can significantly influence flood risk. We obtained the average distance from each analysis unit to the nearest river using Euclidean distance analysis in ArcGIS (Zhang et al., 2016).

2.4. Statistical analysis

2.4.1. Principal component analysis

We employed a Principal Component Analysis (PCA) (Abdi & Williams, 2010) to reduce data dimensionality and extract key features. PCA transforms the original variables into uncorrelated principal components (PCs), effectively mitigating multicollinearity and focusing on the most significant data features (Dai et al., 2023). First, we standardized the influencing factors as PCA is sensitive to variable magnitudes. Next, we calculated the covariance matrix to assess the linear relationships between variables. The eigenvalues of the covariance matrix, representing the variance explained by each principal component (PC), were plotted in a scree plot, and the elbow method was used to determine the optimal number of components to retain (Schreiber, 2021). The data were then transformed into the new feature space defined by the PCs, effectively reducing dimensionality while preserving most of the variance. Finally, we checked the proportion of variance explained by the retained components to ensure that the reduced feature set captured most of the original data's variability.

We interpreted the PCs by examining their factor loadings. Variables with absolute loadings > 0.55 were considered significant and retained for further analysis. Loadings indicate the contributions of a variable to a specific PC, with higher values signifying a stronger influence. The sign

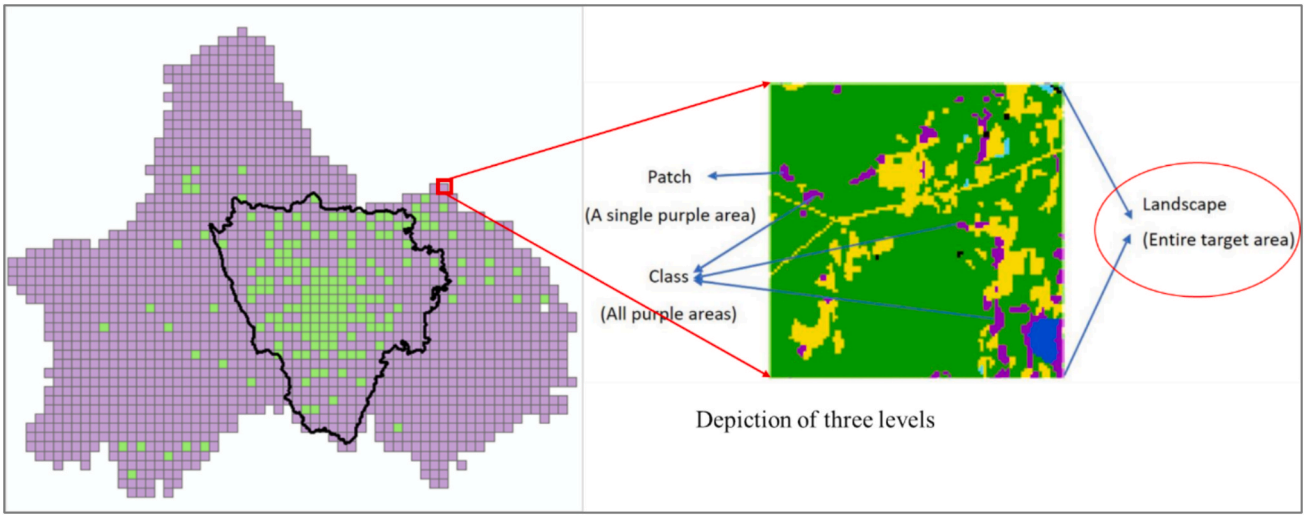

Fig. 4. A conceptual diagram that illustrates the relationship between patch, class, and landscape.

Table 2
Summary and description of flood influencing factor used in the study.

Variable	Formula	Description (Unit)
Landscape composition factors		
P_i	$P_i = \frac{\sum_{j=1}^{n_i} a_{ij}}{A}$	Percentage of land cover i (P_i) within an analysis unit.
PR	$PR = n_i$	Patch Richness (PR), the number of different patch types within an analysis unit.
Landscape configuration factors		
LPI	$LPI = \frac{\max(a_{ij})}{A}(100)$	The Largest Patch Index (LPI), representing the percentage of the landscape unit occupied by the largest patch.
TE	$TE = \sum_{i=1}^{m}\sum_{j=1}^{n_i} e_{ij}$	Total Edge (TE), which is the sum of the lengths of all edge segments.
ED	$ED = TE/A$	Edge Density (ED), defined as the total edge in the landscape unit divided by the total landscape area.
$AREA_m$	$AREA_m = \frac{\sum_{i=1}^{m}\sum_{j=1}^{n_i} a_{ij}}{N}$	Mean Patch Area (*AREAm*), the average area of the corresponding patches within an analysis unit
$SHAPE_m$	$SHAPE_m = \frac{0.25P_i}{n\sqrt{a_i}}$	Average shape index of the corresponding patches within an analysis unit.
LSI	$LSI = \frac{0.25TE}{\sqrt{A}}$	Landscape Shape Index (LSI), reflecting changes in patch shape within an analysis unit.
PD	$PD = \frac{N}{A}$	Patch Density (PD), expressing the number of patches per unit area.
SHDI	$SHDI = -\sum_{i=1}^{m}(P_i \bullet \ln P_i)$	Shannon's Diversity Index, reflecting landscape diversity, complexity, and heterogeneity.
DIVISION	$DIVISION = 1-\sum_{i=1}^{m}\sum_{j=1}^{n_i}(\frac{a_{ij}}{A})^2$	Division Index (DIVISION), indicating the probability that two randomly chosen pixels are not situated in the same patch.
AI	$AI = \left[\sum_{i=1}^{m}\left(\frac{g_{ii}}{\max(g_{ii})}\right)P_i\right]\times 100$	Aggregation Index (AI), quantifying the aggregation degree of patches within an analysis unit.
CONTAG	$CONTAG = \left[1+\frac{\sum_{i=1}^{m}\sum_{k=1}^{m}\left[P_i\left(\frac{g_{ik}}{\sum_{k=1}^{m}g_{ik}}\right)\right]\left[\ln(P_i)\left(\frac{g_{ik}}{\sum_{k=1}^{m}g_{ik}}\right)\right]}{2\ln(m)}\right]\times 100$	Contagion Index (CONTAG), measuring the extent to which landscape elements are aggregated or dispersed.
COHESION	$COHESION = (100)\times\left[1-\frac{\sum_{j=1}^{n}p_{ij}}{\sum_{j=1}^{n}p_{ij}\sqrt{a_{ij}}}\right]\times\left[1-\frac{1}{\sqrt{Z}}\right]^{-1}$	Cohesion Index (COHESION), indicating the physical connectedness of the corresponding patch type.
Topographic factors		
E_m	–	Mean elevation value within an analysis unit.
E_r	$E_r = E_{max} - E_{min}$	Elevation range within an analysis unit.
S_m	–	Mean slope value within an analysis unit.
S_r	$S_r = S_{max} - S_{min}$	Slope range within an analysis unit.
C_m	–	Mean curvature value within an analysis unit.
C_r	$C_r = C_{max} - C_{min}$	Curvature range within an analysis unit.
Hydrological factor		
DisRIVERm	–	Average distance to the river network

N = the total number of patches, A = total landscape area, m= 8 means the total number of patch types, i indicates the ith patch type ($i \le m$), n_i = the total number of the ith patch type, j represent the jth patch in ith patch type, a_{ij} = area of patch ij, P_i = the proportion of the landscape occupied by patch type i, e_i = the length of edge involving patch type i, g_{ik} = the total number of times that patch type i adjacent to type k, g_{ii} = the number of like adjacencies (joins) between pixels of patch type i based on the single-count method, $\max(g_{ii})$ = the maximum number of like adjacencies (joins) between pixels of patch type i based on the single-count method and P_i = proportion of the landscape comprised of patch type i.

of a loading reflects the direction of the relationship: a positive loading indicates a direct association with the PC, whereas a negative loading indicates an inverse association.

2.4.2. Stepwise Poisson regression model

We used a stepwise Poisson regression model to capture the relationship between flooding occurrences and the influencing factors from PCA (Neri et al., 2020). A stepwise procedure allowed us to select those components that have the most influence on the response variable. Here, the count of flood events serves as the response variable, while the influencing factors described in section 2.3 act as predictor variables. We adopted a forward selection procedure, starting with an empty model that only included the intercept. Variables were added step by step, until no further improvement in model fit was achieved. During this process, the procedure also checked whether the inclusion of a new variable rendered any previously added variables redundant, in which case those variables were removed. Through this iterative approach, variables were added or removed to optimize the model's goodness of fit. Our model assumes that the number of flood occurrences per cell is a realization from the Poisson distribution whose intensity λ_i is expressed as:

$$log(\lambda_i) = log(\|\alpha_i\|) + \beta_0 + \sum_{k=1}^{K}\beta_k x_{ik} \# \quad (1)$$

where λ is the expected number of the flooding reporting points at each observation cell, β_0 is the intercept, β_k is the coefficients for the influencing factor x_k, K is the number of selected variables, $\log(\|\alpha_i\|)$ is an offset term to adjust for scale effect, where $\|\alpha_i\|$ represents the area of the cell. By incorporating this $\log(\|\alpha_i\|)$, we adjust for the fact that larger areas are more likely to have more flooding events simply due to their size. This ensures that the model accounts for scale differences between observation units, focusing on the true relationship between the influencing factors and flooding occurrence.

3. Results

3.1. Determining the number of principal components

The scree plots with parallel analyses at scale levels S1, S2, and S3 (Fig. 5) indicate that the first PC shows a notably high eigenvalue—7.28 for S1, 7.72 for S2, and 7.3 for S3—followed by a sharp decline. This suggests that the first PC alone accounts for approximately 30 % of the total variance across the three scales. The first eight PCs have eigenvalues greater than 1, signifying that they capture the most significant variance in influencing factors and are, therefore, considered important for retention. considered significant and worth retaining. Notably, the cumulative explained variance of the first eight PCs are larger than 80 %, suggesting that they can effectively summarize the influencing factors.

3.2. Exploring analysis at S1

3.2.1. Principal components at S1

The Sankey diagram in Fig. 6 illustrates the contributions of various influencing factors to the PCs at the 1 km planning scale. Each factor's contribution to a PC is represented by the value in parentheses, which indicates the loading of that factor on the respective PC.

PC1 is entirely composed of landscape configuration factors, while PC2 is mainly influenced by topographic factors. This indicates that, at the 1 km scale, landscape configuration factors are the primary variables to consider, followed by topographic factors. PC1 shows high positive loadings for ED, LSI, TE, SHDI, and DIVISION, indicating a strong positive correlation among these factors. These five factors primarily

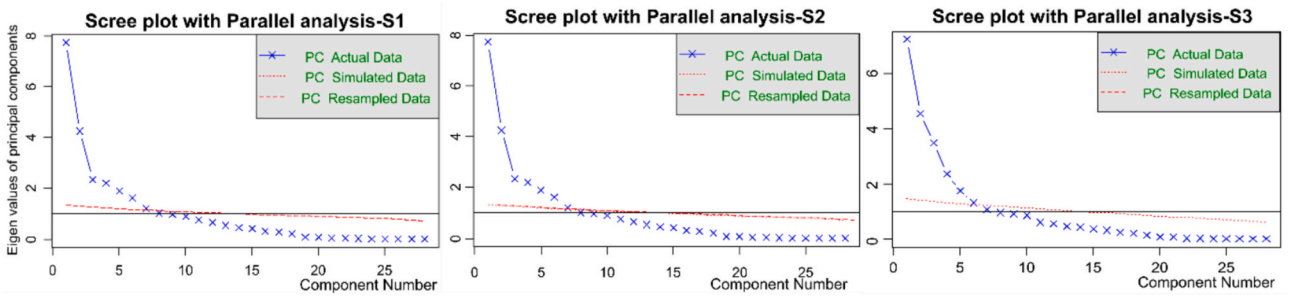

Fig. 5. Scree plot at the three scale levels. The horizontal axis represents the principal component numbers and the vertical axis the eigenvalues.

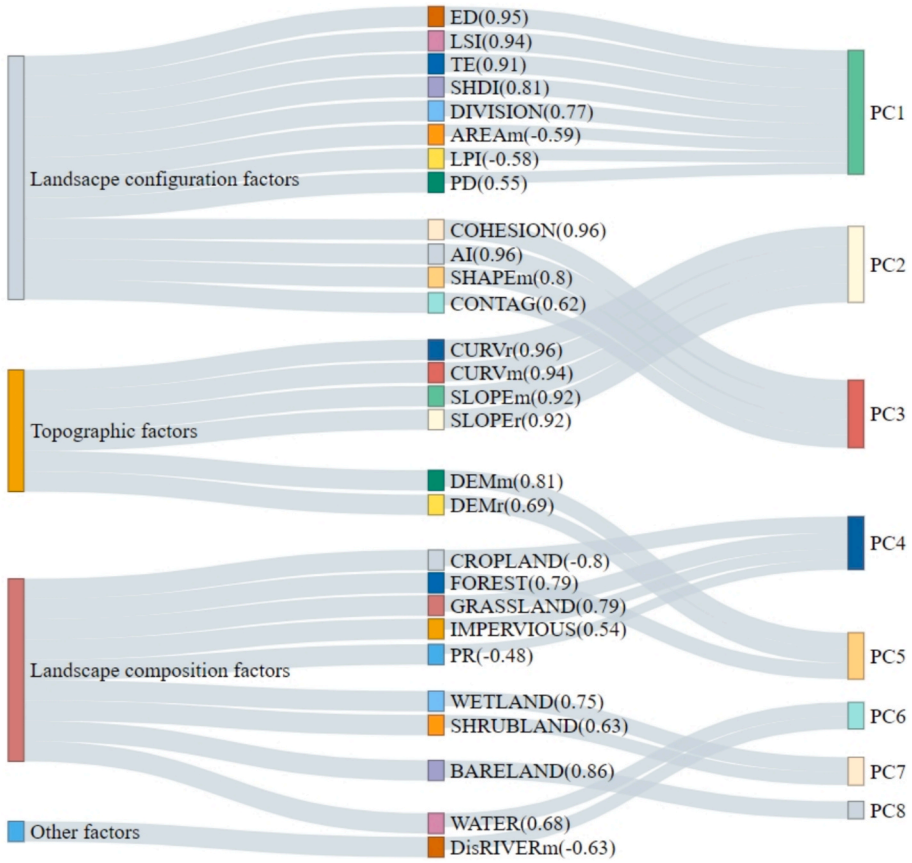

Fig. 6. Factor loadings of flood influencing factors on PCs at S1, with standardized loading values shown in parentheses.

represent landscape diversity. In contrast, AREAm and LPI have high negative loadings, reflecting aggregation patterns. Together they explain a large portion of the variance in the data related to landscape configuration. PC3 is largely explained by COHESION (0.96). PC4 captures the variance explained by the landscape composition. PC5 mainly reflects the influence of topographic factors, especially DEMm (0.81). PC6-8 shows the influence of different types of landscape composition.

3.2.2. *Poisson regression analysis at S1*

Fig. 7 shows the estimated coefficients for each PC with their 95 % confidence intervals. An increase in PC1 (Landscape edge & shape) and PC2 (Slope & Curvature) is associated with an increase in flood occurrences. While PC3 (landscape contagion) and PC4 (landscape composition) are negatively related with flood events. The coefficient for PC5 (Elevation factors) is approximately −1.1, the largest in absolute value, suggesting that the DEM-dominated PC5 has the greatest influence on flood events, with lower elevations leading to more flood occurrences. The confidence interval for PC7 includes zero, indicating that it is not statistically significant. PC7 is composed of wetland and shrubland, suggesting that these landscape compositions have a minimal impact on flooding.

3.3. *Exploring analysis at S2*

3.3.1. *Principal components at S2*

The PCA results for S2 are depicted in Fig. 8, indicate that at the 2 km planning scale, landscape configuration factors are the primary contributors to data variance, as they dominate both PC1 and PC2. In contrast, PC3 and PC4 are more influenced by topographic and landscape composition factors. This suggests that landscape configuration factors explain the majority of variance at this scale, making them the most critical variables to consider, followed by topographic and then landscape composition factors. Specifically, PC1 is strongly associated with factors such as DIVISION (0.87), SHDI (0.8), LPI (−0.87), and CONTAG (−0.71), highlighting their significant role in data variability. PC2 shows high positive loadings for LSI, TE, and ED, suggesting a

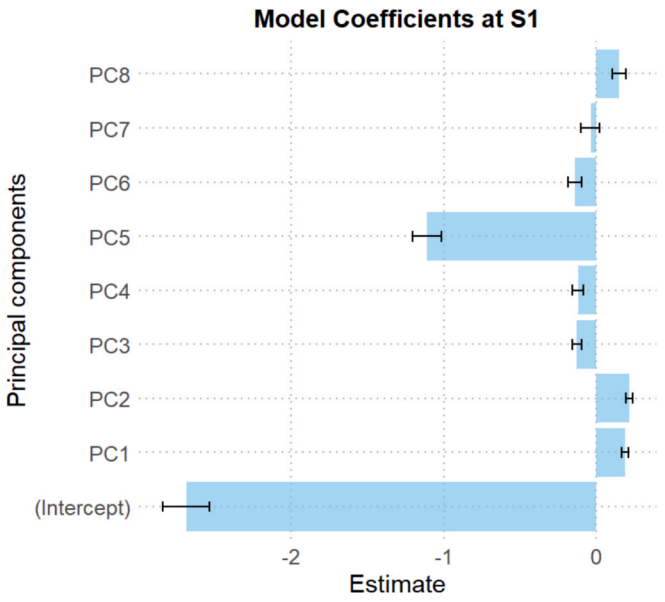

Fig. 7. Poisson regression model coefficients with 95% confidence intervals at S1.

positive correlation among these factors, which contribute to a similar variance pattern. Conversely, AI and AREAm are inversely correlated with PC2. Additionally, PC5 is primarily driven by COHESION, PC6 is associated with curvature, and PC 7 and PC8 reflect landscape composition, particularly wetlands and bare land.

3.3.2. *Poisson regression analysis at S2*

The Poisson regression coefficients for S2 was shown in Fig. 9. PC1 (landscape division) and PC3 (slope) display negative correlations with urban floods, indicating that greater landscape division and steeper slopes potentially mitigate flood risks at S2. In contrast, the positive coefficient of PC2 highlights that larger patches in landscape units contribute positively to the occurrence of urban floods. PC4, representing landscape composition factors with a focus on impervious areas, shows the strongest positive coefficient (approximately 0.88). This suggests that higher percentages of impervious areas significantly increase the frequency of flooding events. Moreover, PC5-7 also has a positive coefficient for flooding events, which indicating the landscape connection factors and curvature may increase the flood risk. PC8, which consists of bareland and shrubland, is not statistically significant, indicating that these two landscape compositions have rarely influence on flooding.

3.4. *Exploring analysis at S3*

3.4.1. *Principal components at S3*

Fig. 10 shows the PCA results at 3-km planning scale. PC1 is composed of topographic factors, while PC2 consists of landscape configuration factors. This suggests that, at the S3 scale, topographic factors account for the most data variance, followed by landscape configuration factors. In PC1, the positive loadings for slope and curvature suggest that as these factors increase, the score for PC1 also rises. In PC2, LPI (−0.95) and DIVISION (0.94) have the highest loadings, indicating that PC2 captures the landscape's division and fragmentation. PC3 consists of PD and AI, with PD representing the patch density of the landscape. PC4-7 are composed from various sources of influencing factors. Based on the factor loadings, PC4 is dominated by landscape composition, PC5 by DEM, PC6 by landscape shape, and PC7 and PC8

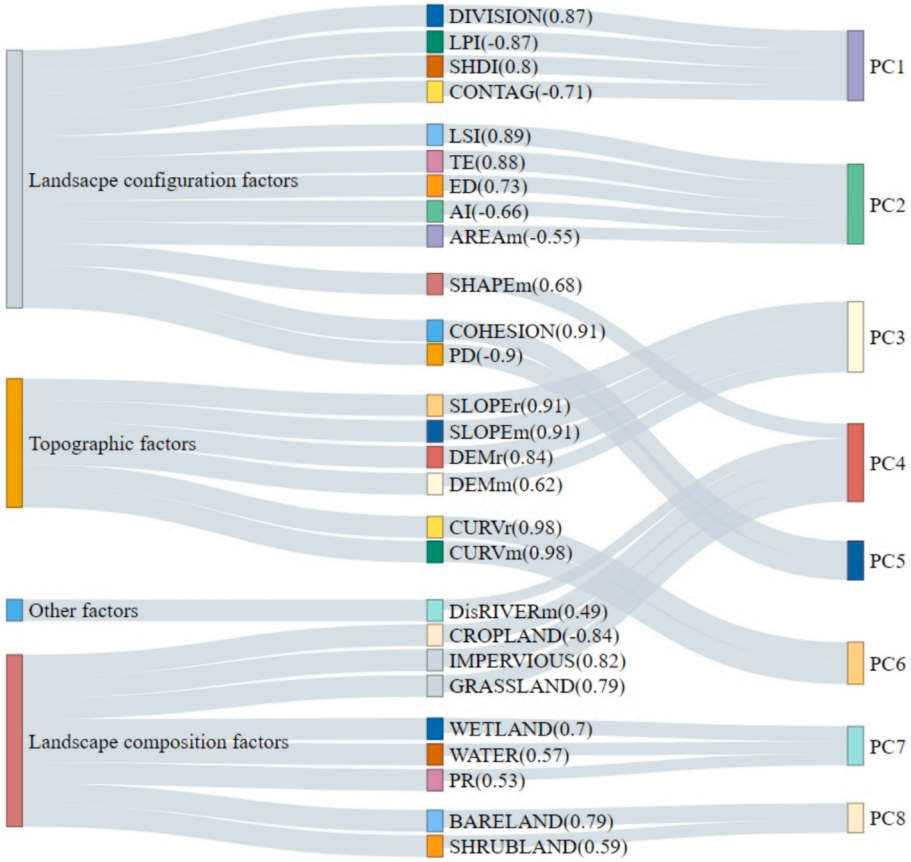

Fig. 8. Factor loadings of flood influencing factors on PCs at S2, with standardized loading values shown in parentheses.

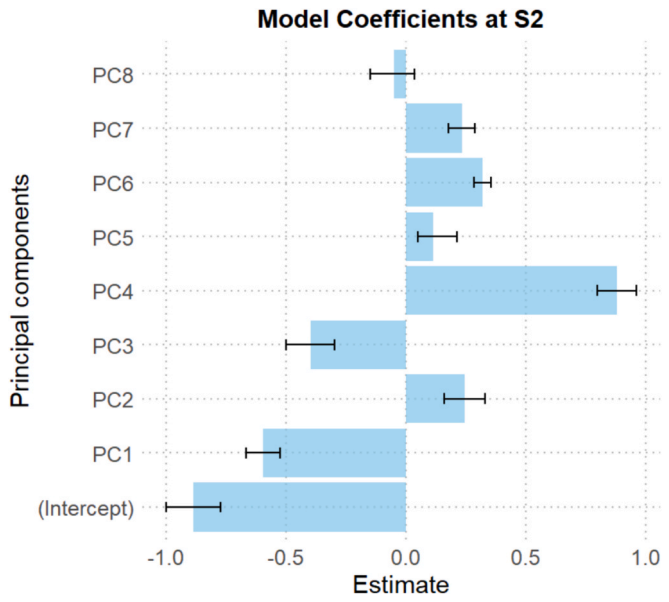

Fig. 9. Poisson regression model coefficients with 95% confidence intervals at S2.

are primarily influenced by water and bareland, respectively.

3.4.2. *Poisson regression analysis at S3*

The negative coefficients for PC1, PC2, PC3, and PC5 imply the increase of these factors will contribute to a decrease in flood occurrences at this scale (Fig. 11). Among these, PC2 (landscape configuration factors) has the highest absolute value (0.41) of coefficients, meaning more diversity and division of the landscape will decrease the flood occurrences. PC5 could reflect the landscape composition factors, with increases in impervious area being significantly associated with higher flood risk. PC8, which consists of bare land, is not statistically significant, indicating it exert little influence on flooding.

3.5. *Stepwise Poisson regression analysis on the original factors*

Table 3 presents the coefficient estimates (with standard errors) from stepwise Poisson regression models. Variables with p-value ≤ 0.05 are considered significant for the regression model. Several influencing factors were found to significantly influence urban flood events across all three spatial scales (S1, S2, and S3).

For landscape configuration factors, AREAm and COHESION are significant at all three scales. Specifically, AREAm is significantly negatively correlated with flood events at all three scales, indicating that more dispersed patches are associated with fewer flood events. In contrast, COHESION shows a significant positive correlation with flooding at all three scales. In model S1, an increase of one unit in the COHESION index is associated with an expected increase of approximately 2.07 flooding events, holding all other variables constant.

For terrain factors, SLOPEr and CURVr are significant in all three regression models. SLOPEr exhibits mixed effects across different scales: in S1 and S3, the coefficients are positive, suggesting that steeper slopes increase flood risk, whereas in S2, the coefficient is negative, implying that relative slope decreases flood risk. Similarly, CURVr also shows varying effects across scales. The negative coefficients in S1 and S3 suggest that areas with higher curvature are less prone to flooding.

DisRIVERm is significantly negatively correlated with flooding at all three scales, indicating that areas closer to rivers are more prone to flooding.

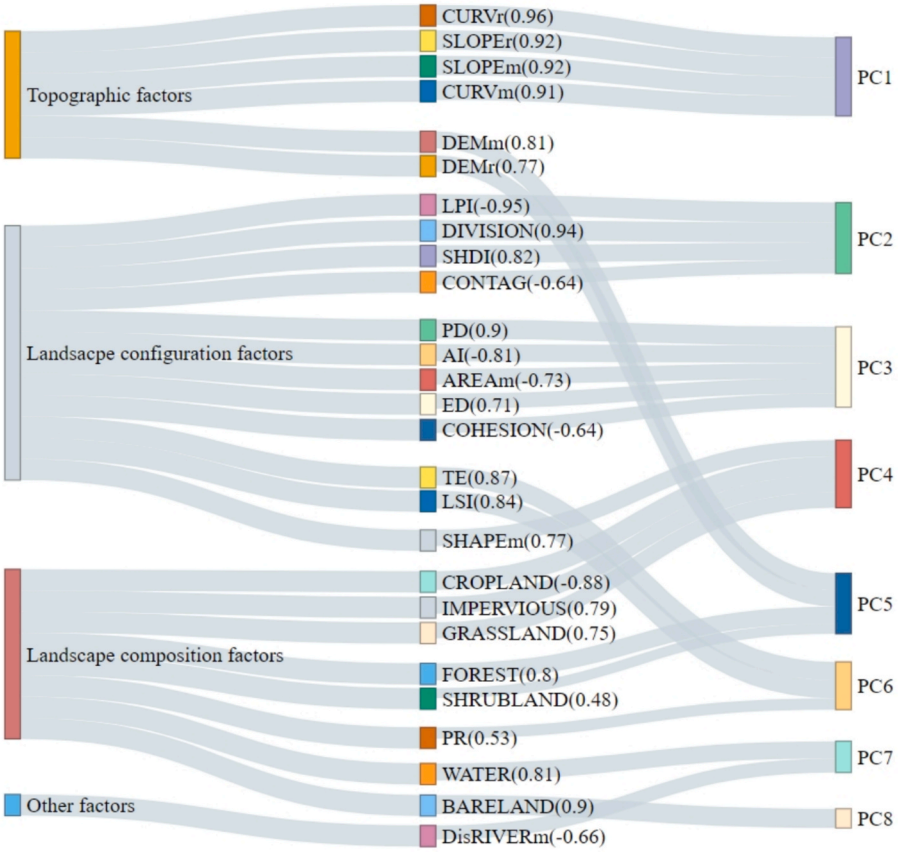

Fig. 10. Factor loadings of flood influencing factors on PCs at S3, with standardized loading values shown in parentheses.

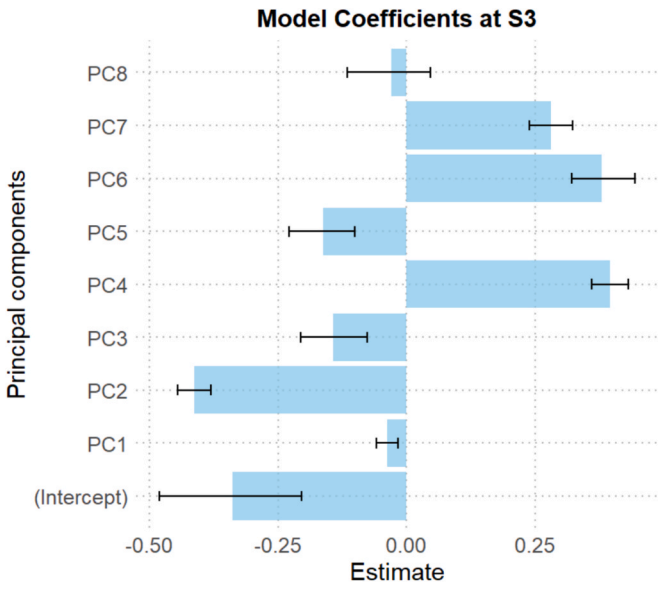

Fig. 11. Poisson regression model coefficients with 95% confidence intervals at S3.

4. Discussion

4.1. The influence of landscape patterns on urban flooding

Currently, several studies have been carried out on the effect of landscape on water flows. For example, Liu et al. (2020) investigated the relationship between the landscape pattern and hydrological flows, but the effect of landscape on urban flood events still remains unclear (Diakakis et al., 2017). Our study found landscape configuration had a more significant impact to flood events than landscape composition, which has similar patterns to Liu et al. (2020)'s conclusion: in sub-tropical catchments, landscape pattern has more effect on hydrological flows than landscape composition. The regression results showed that the division landscape group always show negative influence on urban flood events. We have noticed that the PCA results categorized the landscape configuration as three groups: division & complexity, connection & aggregation, and shape & size. These results confirm the existing evidence in Nowosad and Stepinski (2018) who showed that two type of variables – complexity and aggregation can explain 70 % of the variability of geometric landscape configurations globally.

Specific landscape configuration factors: COHESION and AREAm were significantly correlated with flooding across all scales. The positive regression coefficient for COHESION indicates that higher COHESION values—representing more connected and continuous landscape patches—can increase flooding risk. This is consistent with Zhang et al. (2020)'s findings, which showed that the aggregation of impervious surfaces amplifies urban flooding events. In contrast, AREAm was negatively correlated with flooding. Larger patch areas often have a dominant patch, reflect more natural surfaces with more green space, thereby reducing flood risk (Peng et al., 2019).

4.2. Scale effects

Our findings exhibit strong scale effects, and we recommend that each scale should be given specific focus depending on the stage of planning or the scale of analysis. Previous research (Zhang et al., 2020b) has also demonstrated that the explanatory power of a given factor can vary across different scales, sometimes even reversing the direction of correlation. Although this can lead to contradictory or challenging interpretations of results, it also underscores the necessity of multi-scale studies. Especially in the field of planning and management, different scales can reveal varying levels of information, as highlighted by Liu et al. (2020).

Our study suggests that when considering scale effects, attention should be paid to three key aspects: (1) **The diversity of landscape patterns**: at larger scales, the diversity of landscape composition increases, encompassing various land uses and covers, such as urban buildings, green spaces, and water bodies. This diversity has a more pronounced impact on hydrological responses, as different landscape types influence interception, infiltration, and runoff differently. In smaller-scale areas, landscape types may be more uniform, and their impact may be relatively minor. (2) **Statistical aspects**: in statistical analysis, the sample size and range of variability significantly affect the

Table 3
Stepwise Poisson regression results for influencing factors at different scales.

		Coefficient Estimate (std error)		
	Factors	**S1 model**	**S2 model**	**S3 model**
	(Intercept)	−3.034***(0.146)	−4.342***(1.094)	−5.516***(1.094)
Landscape configuration	PD	−1.655***(0.243)	−1.238***(0.364)	
	TE	4.633*(2.219)	−10.186(6.397)	−18.486***(7.589)
	LPI		−0.413***(0.124)	
	ED		−12.044·(6.829)	−20.269*(8.173)
	LSI	−3.87·(2.189)	21.863·(12.89)	38.055*(15.168)
	AREAm	−1.18***(0.155)	−1.03***(0.149)	−0.242*(0.058)
	SHAPEm	−0.68***(0.155)		
	CONTAG	−0.535***(0.122)		2.261***(0.652)
	COHESION	2.071**(0.711)	1.558***(0.403)	0.899**(0.274)
	DIVISION	0.186(0.118)		
	PR	0.18*(0.084)		−0.674***(0.199)
	SHDI	−0.851***(0.142)	−0.151·(0.083)	1.962***(0.526)
Topographic factors	DEMm	−0.42***(0.115)		
	DEMr	0.96***(0.151)		−0.668***(0.143)
	SLOPEm	−13.763**(5.207)	−8.327*(2.652)	
	SLOPEr	13.331**(5.117)	−5.516***(1.094)	−0.364***(0.089)
	CURVm	0.88***(0.148)	NA	
	CURVr	−1.044***(0.192)	−0.134***(0.024)	−0.207***(0.061)
Hydrological factors	DisRIVERm	−0.24***(0.038)	−0.194***(0.038)	−0.278***(0.038)
Landscape composition	VEGETATION			20.87***(5.788)
	WATER		0.216***(0.032)	2.064***(0.558)
	IMPERVIOUS		1.137***(0.05)	22.001***(5.797)

Note: Signif. codes: ***(p < 0.001), ** (p < 0.01), *(p < 0.05),· (p < 0.1), (p > 0.1); NA: Variables not selected. Highlighted factors significantly influencing urban flood events across all three spatial scales.

significance of results. Larger-scale areas provide more data points and a broader range of variability, potentially enhancing the statistical model's ability to detect significant relationships. When the study area and sample size are fixed, however, using overly large study units may result in an insufficient number of samples, while using overly small units could lead to each unit containing too few data points. This imbalance can make it challenging to demonstrate statistically significant relationships. (3) **Efficiency and Computational Power**: as scale increases in resolution, the processing power and computation time required also increase. Finer scales demand more computational resources and time, as noted by (Fewtrell et al., 2008).

4.3. Implications for urban flooding reduction

By means of a PCA and a stepwise Poisson regression analysis of 28 influencing factors, we identified several key indicators that can be used to reduce urban flooding.

From a landscape perspective, a more dispersed spatial pattern and greater diversity in landscape compositions consistently reduce the occurrence of flooding across all scales. Additionally, decreasing the proportion of impervious surfaces is an effective strategy. Therefore, we recommend that urban planning prioritize maintaining a sufficient proportion of green spaces and ensure that impervious areas are more spatially dispersed distributed.

From the topographic perspective, several factors show different effect on flooding events. At smaller scales (1 km), areas with higher slopes are more effective in mitigating flood events. Therefore, we suggested constructing sunken catchment areas could be beneficial at this scale. In contrast, at larger scales, maintaining relatively flat terrain is advisable; however, low-lying areas tend to be more prone to water accumulation. This aligns with previous studies (Zhang et al., 2020a), which suggest that in low-lying areas, the elevation of sunken green spaces or roadbeds should be 5–30 cm lower than the surrounding surface to increase slope and reduce flooding risk.

From the hydrological perspective, areas near rivers are more susceptible to flooding. This increased risk is likely because many drainage systems are connected to rivers, and during the rainy season, rising river levels can impede drainage, leading to potential backflow and even overflow of riverbanks. Therefore, we suggested that urban planning in river-adjacent areas should prioritize the development of water retention spaces. These spaces can mitigate urban flooding by reducing surface runoff through infiltration, detention, and storage.

Based on these findings, we propose scale-specific flood mitigation strategies. At the 1 km scale (S1), where steeper slopes help reduce flooding, planning should focus on localized drainage improvements such as micro-catchment designs, permeable pavements, and small-scale green infrastructure to enhance runoff management. At the 2 km scale (S2), where impervious surface expansion is the main driver, efforts should control urban sprawl and integrate stormwater management systems. At the 3 km scale (S3), where landscape configuration dominates, enhancing green corridors and maintaining landscape connectivity are critical for regulating water flow and reducing urban flood.

4.4. Limitations and future directions

This study provides insights into the impact of landscape patterns on urban flooding, but several limitations should be acknowledged. First, regarding data availability, the flood records used in this study were primarily sourced from social media, which may be spatially inconsistent. Future studies could integrate multiple data sources, such as citizen science records, remote sensing observations, and hydrological model simulations, to enhance data comprehensiveness and reliability. Second, in terms of modeling, stepwise Poisson regression effectively identifies key influencing factors, but it has some limitations in capturing nonlinear relationships and complex interactions between variables. Future research could explore the application of machine learning methods or spatial statistical models to enhance predictive performance. We further realize that this study primarily focused on surface landscape characteristics without explicitly considering the role of underground drainage systems. Urban flooding, however, results from an interplay between surface runoff and drainage capacity. This highlights the need for future studies to integrate surface landscape patterns with subsurface drainage networks for a more comprehensive flood risk assessment. Lastly, as this study was conducted in the urbanized area of Chengdu, generalizing our findings to other urban areas or to non-urban areas may be limited. Hence, future studies might benefit from integrating multi-source data, adopt spatial statistical models, and incorporate urban hydrodynamic models to refine and assess urban flood risks. This will ultimately support more informed decision-making in urban planning and flood management.

5. Conclusion

The key findings of this study are summarized as follows:

(1) The significance of environmental factors to the PCs varied across scales. According to the PCA, landscape configuration accounted for the major variance at the 1 km and 2 km planning scales, while at the 3 km scale, topographic factors were the primary contributors. The Poisson regression results showed that each scale contained dominant factor: at the 1 km scale, topographic factors had the highest regression coefficient (−1.1); at the 2 km scale, factors dominated by impervious areas had the largest coefficient (0.88); and at the 3 km scale, landscape configuration factors had the most significant impact (−0.41).

(2) The study shows that more fragmented and dispersed landscapes tend to decrease the occurrence of floods. In contrast, landscapes with high connectivity and aggregation, as well as those with extensive impervious surfaces, are associated with an increased flood risk. Distance to rivers plays a critical role, with areas farther from rivers experiencing less flooding. Topographic influences showed that the DEM was negatively correlated with flooding across all scales, whereas slope and curvature exhibited a positive correlation at the 1 km scale, shifting to a negative correlation at larger scales.

(3) In the single-factor regression analysis, both AREAm and COHESION were significant at all three scale levels. Specifically, AREAm was significantly negatively correlated with flooding, indicating that larger mean patch areas are associated with less flooding. Conversely, COHESION showed a significant positive correlation with flooding at all scales, suggesting that more dispersed patches are linked to fewer flood events.

(4) Our multi-scale analysis provides theoretical guidance for urban planners in urban flooding management. It underscores the varying importance of landscape pattern and topographic factors in flood risk management. In this way, it highlights the need for scale-specific strategies in urban planning and flood mitigation.

CRediT authorship contribution statement

Yao Li: Writing – original draft, Conceptualization. **Frank Badu Osei:** Writing – review & editing, Visualization. **Shaoqing Dai:** Writing – review & editing, Visualization. **Tangao Hu:** Writing – review & editing, Investigation, Data curation. **Alfred Stein:** Writing – review & editing, Supervision, Conceptualization.

Declaration of competing interest

The authors declare that they have no known competing financial interests or personal relationships that could have appeared to influence the work reported in this paper.

Acknowledgements

This work was supported by the "Pioneer and Leading Goose + X" S&T Program of Zhejiang (Grant No. 2025C02230), the National Natural Science Foundation of China (Grant No. 42471102), and a Fellowship from the China Scholarship Council (Grant No. 202008330335).

Data availability

Data will be made available on request.

References

Abdi, H., Williams, L.J., 2010. Principal component analysis. *Wires Computational Statistics* 2 (4), 433–459. https://doi.org/10.1002/wics.101.

Ali, A., Rana, I.A., Ali, A., Najam, F.A., 2022. Flood risk perception and communication: The role of hazard proximity. *Journal of Environmental Management* 316, 115309. https://doi.org/10.1016/j.jenvman.2022.115309.

Birkholz, S., Muro, M., Jeffrey, P., Smith, H.M., 2014. Rethinking the relationship between flood risk perception and flood management. *Science of the Total Environment* 478, 12–20. https://doi.org/10.1016/j.scitotenv.2014.01.061.

Chen, W., Wang, W., Huang, G., Wang, Z., Lai, C., Yang, Z., 2021. The capacity of grey infrastructure in urban flood management: A comprehensive analysis of grey infrastructure and the green-grey approach. *International Journal of Disaster Risk Reduction* 54, 102045. https://doi.org/10.1016/j.ijdrr.2021.102045.

Dai, S., Zhao, W., Wang, Y., Huang, X., Chen, Z., Lei, J., Stein, A., Jia, P., 2023. Assessing spatiotemporal bikeability using multi-source geospatial big data: A case study of Xiamen, China. *International Journal of Applied Earth Observation and Geoinformation* 125, 103539. https://doi.org/10.1016/j.jag.2023.103539.

Davis, M., Naumann, S., 2017. Making the Case for Sustainable Urban Drainage Systems as a Nature-Based Solution to Urban Flooding. In: Kabisch, N., Korn, H., Stadler, J., Bonn, A. (Eds.), *Nature-Based Solutions to Climate Change Adaptation in Urban Areas: Linkages between Science, Policy and Practice*. Springer International Publishing, pp. 123–137. https://doi.org/10.1007/978-3-319-56091-5_8.

Diakakis, M., Deligiannakis, G., Pallikarakis, A., Skordoulis, M., 2017. Identifying elements that affect the probability of buildings to suffer flooding in urban areas using Google Street View. A case study from Athens metropolitan area in Greece. *International Journal of Disaster Risk Reduction* 22, 1–9. https://doi.org/10.1016/j.ijdrr.2017.02.002.

Fewtrell, T.J., Bates, P.D., Horritt, M., Hunter, N.M., 2008. Evaluating the effect of scale in flood inundation modelling in urban environments. *Hydrological Processes* 22 (26), 5107–5118. https://doi.org/10.1002/hyp.7148.

Gong, P., Li, X., Wang, J., Bai, Y., Chen, B., Hu, T., Zhou, Y., 2020. Annual maps of global artificial impervious area (GAIA) between 1985 and 2018. Remote Sensing of Environment 236, 111510. https://doi.org/10.1016/j.rse.2019.111510.

Karimi, J.D., Corstanje, R., Harris, J.A., 2021. Understanding the importance of landscape configuration on ecosystem service bundles at a high resolution in urban landscapes in the UK. *Landscape Ecology* 36 (7), 2007–2024. https://doi.org/10.1007/s10980-021-01200-2.

Kuo, P.-H., Shih, S.-S., Otte, M.L., 2021. Restoration recommendations for mitigating habitat fragmentation of a river corridor. *Journal of Environmental Management* 296, 113197. https://doi.org/10.1016/j.jenvman.2021.113197.

Li, J., Zhou, K., Xie, B., Xiao, J., 2021. Impact of landscape pattern change on water-related ecosystem services: Comprehensive analysis based on heterogeneity perspective. *Ecological Indicators* 133, 108372. https://doi.org/10.1016/j.ecolind.2021.108372.

Li, J., Bortolot, Z.J., 2022. Quantifying the impacts of land cover change on catchment-scale urban flooding by classifying aerial images. Journal of Cleaner Production 344, 130992. https://doi.org/10.1016/j.jclepro.2022.130992.

Li, Y., Osei, F.B., Hu, T., Stein, A., 2023a. Urban flood susceptibility mapping based on social media data in Chengdu city, China [Article]. *Sustainable Cities and Society* 88, 104307. https://doi.org/10.1016/j.scs.2022.104307.

Li, Y., Wang, P., Lou, Y., Chen, C., Shen, C., Hu, T., 2024. Assessing urban drainage pressure and impacts of future climate change based on shared socioeconomic pathways. *Journal of Hydrology: Regional Studies* 53, 101760. https://doi.org/10.1016/j.ejrh.2024.101760.

Li, Y., Ye, S., Wu, Q., Wu, Y., Qian, S., 2023b. Analysis and countermeasures of the "7.20" Flood in Zhengzhou. *Journal of Asian Architecture and Building Engineering* 22 (6), 3782–3798.

Liu, J., Liu, X., Wang, Y., Li, Y., Jiang, Y., Fu, Y., Wu, J., 2020. Landscape composition or configuration: which contributes more to catchment hydrological flows and variations? *Landscape Ecology* 35 (7), 1531–1551. https://doi.org/10.1007/s10980-020-01035-3.

Ma, S., Li, Y., Zhang, Y., Wang, L.-J., Jiang, J., Zhang, J., 2022. Distinguishing the relative contributions of climate and land use/cover changes to ecosystem services from a geospatial perspective. *Ecological Indicators* 136, 108645. https://doi.org/10.1016/j.ecolind.2022.108645.

Ma, X., Zhang, P., Yang, L., Qi, Y., Liu, J., Liu, L., Fan, X., Hou, K., 2024. Assessing the relative contributions, combined effects and multiscale uncertainty of future land use and climate change on water-related ecosystem services in Southwest China using a novel integrated modelling framework. *Sustainable Cities and Society* 106, 105400. https://doi.org/10.1016/j.scs.2024.105400.

Nearing, G., Cohen, D., Dube, V., Gauch, M., Gilon, O., Harrigan, S., Hassidim, A., Klotz, D., Kratzert, F., Metzger, A., Nevo, S., Pappenberger, F., Prudhomme, C., Shalev, G., Shenzis, S., Tekalign, T.Y., Weitzner, D., Matias, Y., 2024. Global prediction of extreme floods in ungauged watersheds. *Nature* 627 (8004), 559–563. https://doi.org/10.1038/s41586-024-07145-1.

Neri, A., Villarini, G., Napolitano, F., 2020. Statistically-based projected changes in the frequency of flood events across the US Midwest. *Journal of Hydrology* 584, 124314. https://doi.org/10.1016/j.jhydrol.2019.124314.

Nowosad, J., Stepinski, T.F., 2018. Global inventory of landscape patterns and latent variables of landscape spatial configuration. *Ecological Indicators* 89, 159–167. https://doi.org/10.1016/j.ecolind.2018.02.007.

Osborne, P.E., Alvares-Sanches, T., 2019. Quantifying how landscape composition and configuration affect urban land surface temperatures using machine learning and neutral landscapes. *Computers, Environment and Urban Systems* 76, 80–90. https://doi.org/10.1016/j.compenvurbsys.2019.04.003.

Pan, Z., Gao, G., Fu, B., Liu, S., Wang, J., He, J., Liu, D., 2023. Exploring the historical and future spatial interaction relationship between urbanization and ecosystem services in the Yangtze River Basin. China. *JOURNAL OF CLEANER PRODUCTION* 428, 139401. https://doi.org/10.1016/j.jclepro.2023.139401.

Peng, Y., Wang, Q., Wang, H., Lin, Y., Song, J., Cui, T., Fan, M., 2019. Does landscape pattern influence the intensity of drought and flood? *Ecological Indicators* 103, 173–181. https://doi.org/10.1016/j.ecolind.2019.04.007.

Rahimi, E., Barghjelveh, S., Dong, P., 2021. Quantifying how urban landscape heterogeneity affects land surface temperature at multiple scales. Journal of Ecology and Environment 45, 1–13.doi.. https://doi.org/10.1186/s41610-021-00203-z.

Saura, S., Castro, S., 2007. Scaling functions for landscape pattern metrics derived from remotely sensed data: Are their subpixel estimates really accurate? *ISPRS Journal of Photogrammetry and Remote Sensing* 62 (3), 201–216. https://doi.org/10.1016/j.isprsjprs.2007.03.004.

Schreiber, J.B., 2021. Issues and recommendations for exploratory factor analysis and principal component analysis. *Research in Social & Administrative Pharmacy* 17 (5), 1004–1011. https://doi.org/10.1016/j.sapharm.2020.07.027.

Šímová, P., Gdulová, K., 2012. Landscape indices behavior: A review of scale effects. Applied geography 34, 385–394. https://doi.org/10.1016/j.apgeog.2012.01.003.

Sohn, W., Kim, J.-H., Li, M.-H., Brown, R.D., Jaber, F.H., 2020. How does increasing impervious surfaces affect urban flooding in response to climate variability? *Ecological Indicators* 118, 106774. https://doi.org/10.1016/j.ecolind.2020.106774.

Sun, L., Yu, H., Sun, M., Wang, Y., 2023. Coupled impacts of climate and land use changes on regional ecosystem services. *Journal of Environmental Management* 326, 116753. https://doi.org/10.1016/j.jenvman.2022.116753.

Wang, L., Hou, H., Li, Y., Pan, J., Wang, P., Wang, B., Chen, J., Hu, T., 2023a. Investigating relationships between landscape patterns and surface runoff from a spatial distribution and intensity perspective [Article]. *J Environ Manage* 325(Pt B), 116631, 116631. https://doi.org/10.1016/j.jenvman.2022.116631.

Wang, P., Li, Y., Fan, J., Kong, F., Zhang, D., Hu, T., 2023b. Future changes in urban drainage pressure caused by precipitation extremes in 285 cities across China based on CMIP6 models [Article]. *Sustainable Cities and Society* 91, 104404. https://doi.org/10.1016/j.scs.2023.104404.

Wang, Y., Li, C., Liu, M., Cui, Q., Wang, H., Lv, J., Li, B., Xiong, Z., Hu, Y., 2022. Spatial characteristics and driving factors of urban flooding in Chinese megacities. *Journal of Hydrology* 613, 128464. https://doi.org/10.1016/j.jhydrol.2022.128464.

Yin, S., Wang, Y., Lei, C., Zhang, J., 2025. Runoff responses to landscape pattern changes and their quantitative attributions across different time scales in ecologically fragile basins. *Catena* 249, 108716. https://doi.org/10.1016/j.catena.2025.108716.

Zhang, Wu., Z., Zhang, H., Dalla Fontana, G., & Tarolli, P., 2020a. Identifying dominant factors of waterlogging events in metropolitan coastal cities: The case study of Guangzhou. China. *J Environ Manage* 271, 110951. https://doi.org/10.1016/j.jenvman.2020.110951.

Zhang, Q., Wu, Z., Guo, G., Zhang, H., Tarolli, P., 2021. Explicit the urban waterlogging spatial variation and its driving factors: The stepwise cluster analysis model and hierarchical partitioning analysis approach. *Sci Total Environ* 763, 143041. https://doi.org/10.1016/j.scitotenv.2020.143041.

Zhang, Q., Wu, Z., Zhang, H., Dalla Fontana, G., Tarolli, P., 2020b. Identifying dominant factors of waterlogging events in metropolitan coastal cities: The case study of Guangzhou. China. *Journal of Environmental Management* 271, 110951. https://doi.org/10.1016/j.jenvman.2020.110951.

Zhang, Y., Wu, T., Song, C., Hein, L., Shi, F., Han, M., Ouyang, Z., 2022. Influences of climate change and land use change on the interactions of ecosystem services in China's Xijiang River Basin. *Ecosystem Services* 58, 101489. https://doi.org/10.1016/j.ecoser.2022.101489.

Zhang, Y., Xian, C., Chen, H., Grieneisen, M.L., Liu, J., Zhang, M., 2016. Spatial interpolation of river channel topography using the shortest temporal distance. *Journal of Hydrology* 542, 450–462. https://doi.org/10.1016/j.jhydrol.2016.09.022.

Zheng, Q., Shen, S.-L., Zhou, A., Lyu, H.-M., 2022. Inundation risk assessment based on G-DEMATEL-AHP and its application to Zhengzhou flooding disaster. *Sustainable Cities and Society* 86, 104138. https://doi.org/10.1016/j.scs.2022.104138.

Zimmermann, E., Bracalenti, L., Piacentini, R., Inostroza, L., 2016. Urban Flood Risk Reduction by Increasing Green Areas for Adaptation to Climate Change. *Procedia Engineering* 161, 2241–2246. https://doi.org/10.1016/j.proeng.2016.08.822.

Zou, L., Wang, J., Bai, M., 2022. Assessing spatial–temporal heterogeneity of China's landscape fragmentation in 1980–2020. *Ecological Indicators* 136, 108654. https://doi.org/10.1016/j.ecolind.2022.108654.